JOURNAL OF MATERIALS SCIENCE 29 (1994) 2671–2677

Microstructure and mechanical properties of Cr_3C_2 particulate reinforced Al_2O_3 matrix composites

CHEN-TSU FU‡*, JENN-MING WU‡
‡*Department of Materials Science and Engineering National Tsing Hua University Hsinchu, 31015, Taiwan*
AI-KANG LI*
**Material Research Laboratories Industrial Technology Research Institute Hsinchu, 31015, Taiwan*

Al_2O_3 matrix with three grades of Cr_3C_2 particle size (0.5, 1.5 and 7.5 μm) composites were fabricated by a hot-pressing technique. Fully dense compacts with Cr_3C_2 content up to 40 vol % can be acquired at 1400 °C under 30 MPa pressure for 1 h. The flexural strength increases from 595 to 785 Mpa for fine Cr_3C_2 particle (0.5 μm) reinforced Al_2O_3 matrix composites. The fracture strength is significantly dependent on the fracture modes of matrix (intergranular or transgranular). The transgranular fracture with a compressive residual stress gives a high fracture strength of composites. At the same time, the fracture toughness increases from 5.2 MPa $m^{1/2}$ (10 vol % Cr_3C_2) to 8.0 MPa $m^{1/2}$ (30 vol% Cr_3C_2) for the coarse Cr_3C_2 particle (7.5 μm) reinforced Al_2O_3 matrix composites. The toughening effects of incorporating Cr_3C_2 particles into Al_2O_3 matrix originate from crack bridging and deflection. The electrical conductivity and the possibility of electrical discharge machining of these composites were also investigated.

1. Introduction

Monolithic alumina is one of the most popular ceramic materials used in wear and structural applications, based on its excellent physical properties such as high melting temperature, strength, hardness and corrosion resistance. However, the intrinsic brittleness of alumina makes its reliability limited and prevents wider usage. Various remedies have been employed to increase its toughness, including the use of hard ceramic particulate as a reinforcing phase, which has been shown to be very effective in strengthening and toughening alumina [1–4].

Recently, there has been progress in the development of electroconductive ceramic materials [5–7]. These electroconductive and toughened ceramics could be shaped by electrical discharge machining to manufacture complex components, instead of using expensive conventional diamond tools. In order to obtain such ceramics, an electroconductive phase must be dispersed in an insulated ceramic matrix. With the addition of low electrical resistivity ($< 10^{-5}\ \Omega$ cm) transition metal carbides, borides or nitrides (e.g. TiC, TiN or TiB_2) to improve the electroconductivities of non-oxides [5, 6] or Al_2O_3 [6, 7] matrix, good electroconductive ceramic composites have been demonstrated. At the same time, these composites could be used as high-temperature heaters, igniters and so on to extend the applications, in addition to the wear-resistant components and cutting tools.

In addition to the high modulus and electrical conductivity, the Cr_3C_2 constituents possess outstanding high-temperature erosion resistance, at least to 1100 °C, which makes the materials ideally suitable for hot extrusion dies [8]. In this study, the correlations between densification, microstructures, mechanical properties and electrical conductivity of Al_2O_3 matrix composites with the incorporation of $\sim$ 10–40 vol % Cr_3C_2 particles are investigated. The preliminary results of the size effects of Cr_3C_2 particles on microstructures and mechanical properties are also discussed.

2. Experimental procedures

2.1. Raw materials

The Cr_3C_2 powder used was from Herman C. Stark, with a purity of > 99%. Three sizes of Cr_3C_2 particle were used. The mean particle sizes measured by laser diffraction techniques were 7.5 (L), 1.5 (M) and 0.5 μm (S), respectively. The finest particle was obtained by attritor-milled 1.5-μm particle for 48 h. The Al_2O_3 powder (Alcoa A16-SG) had a particle size of 0.3–0.5 μm and purity of > 99.7%.

0022–2461

2.2. Consolidation procedures

The Cr_3C_2 and Al_2O_3 powders were added together with deionized water and then ball-milled for 24 h. The slurry was further homogenized for 15 min using a high-shear ultrasonic dispersing process. The homogenized slurry was dried rapidly with constant agitation on a hot plate. The dried and sieved mixture was uniaxially pre-pressed to form discs of 5 mm in height and 60 mm in diameter. The green compacts were then placed in a boron nitride-coated graphite mould and hot pressed in the temperature range 1200 to 1700 °C in Ar atmosphere, at a pressure of 30 MPa for 1 h.

2.3. Characterization

The dense composite discs were ground and cut along the grinding direction to $3 \times 4 \times 40$-mm bars. All specimens were polished with diamond pastes from 15 down to 3 μm. Each bar to be used for the fracture toughness test was centre-notched to one-third of its thickness using a 0.15-mm-thick diamond blade. The flexural strength was measured through a four-point bending test following the JIS 1601 method [9] and the fracture toughness was evaluated using the single-edge-notched beam (SENB) method. Both were measured at room temperature. The microstructures, fracture surface and interface of the Cr_3C_2/Al_2O_3 were examined by scanning and transmission electron microscopes (SEM and TEM).

The electrical resistivity was measured by the two-terminal method using a high-resistance meter. Gold was vapour-deposited by sputtering on both sides of the rectangular testing bars ($3 \times 4 \times 10$ mm) to form electrodes.

The Al_2O_3 grain size was evaluated by the line-intercepted method after the samples had been etched in hot phosphoric acid.

3. Results and discussions

3.1. Densification and microstructures

Fig. 1 shows the relative density as a function of hot-pressing temperature for Al_2O_3-based composites containing ~ 10–40 vol % Cr_3C_2(M) particles. The

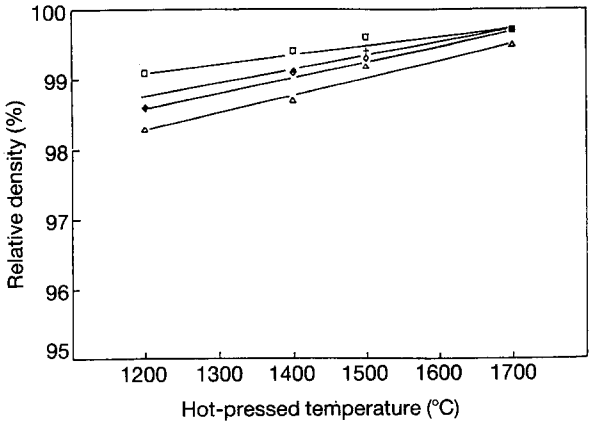

Figure 1 Correlation between relative density and hot-pressed temperature for Al_2O_3 matrix composites incorporated with ~ 10–40 vol % Cr_3C_2 particle size (1.5 μm). □, 10; +, 20; ◇, 30; △, 40%.

densification of Al_2O_3–Cr_3C_2 composites is dependent on the hot-pressing temperature and Cr_3C_2 particle content. A tendency of inhibition of densification of the composite compacts by the Cr_3C_2 additions is clearly observable. Therefore a higher sintering temperature is needed to obtain a fully dense composite with higher Cr_3C_2 particle content. For example, $T \geqslant 1350$ °C for 20 vol % Cr_3C_2, $T \geqslant 1450$ °C for 30 vol % Cr_3C_2, and $T \geqslant 1550$ °C for 40 vol % Cr_3C_2 composites are required to obtain a more than 99% relative density. A reduction in the rate of densification caused by the presence of these rigid inclusions or reinforced second phase is well documented in many theoretical and experimental studies [10–13]. According to their experimental results, the formation of a constrained network [10, 11] and interactions [12] between rigid inclusions will give rise to differential shrinkage characteristics of the matrix and inclusions, and will cause sintering damage such as crack-like flaws or pores. The presence of a second-phase particle will raise the sintering activation energy [13] despite both constant heating rate and isothermal sintering processes. Thus a higher driving force, achieved by raising the temperature, is needed to overcome these obstacles to densification when the Cr_3C_2 content particle is high.

The SEM micrographs observed from the polished surface of dense 30 vol % Cr_3C_2(M)/Al_2O_3 composites sintered at 1400 and 1700 °C are shown in Fig. 2a and b, respectively. The particle size of Cr_3C_2 for composites sintered at 1400 °C is ~ 2 μm, as shown in Fig. 2a, very close to the size of the raw Cr_3C_2 particles. As the sintering temperature rises to 1700 °C, the average particle of Cr_3C_2 is close to 8 μm. The growth of Cr_3C_2 particles is very rapid with the increase of temperature, indicating that Cr_3C_2 must possess sufficient self-diffusion. The main mechanism of Cr_3C_2 particle growth is coalescence. The formation of necks between Cr_3C_2 particles along Al_2O_3 grain boundaries can be seen in Fig. 3. The growth of Cr_3C_2 particles by coalescence proceeded in order to decrease the total surface energy. The morphology of Cr_3C_2 changes from a small spherical single crystal to a large irregular chain-like polycrystalline particle, as illustrated in Fig. 2. The Cr_3C_2/Cr_3C_2 grain boundaries were easily observed after chemical etching, and the different orientation of individual Cr_3C_2 grains within a large irregular particle was also verified by TEM diffraction patterns. The rate of Cr_3C_2 coalescence is a function of sintering temperature and Cr_3C_2 content in the composites. Higher sintering temperature, resulting in a greater diffusivity, and high Cr_3C_2 content giving a shorter mean free path, produce a greater rate of coalescence of Cr_3C_2 particles. Thus for 40 vol % Cr_3C_2/Al_2O_3 composites, some coalescence is affected even when hot-pressed at 1400 °C, because the mean free path is very short.

Fig. 4 indicates that the average grain size of Al_2O_3 is a function of Cr_3C_2 content in composites hot-pressed at various temperatures. There is no grain growth until relative density approaches ~ 90% [14, 15] for a high-purity Al_2O_3 powder with a submicrometre diameter in the initial sintering stage.

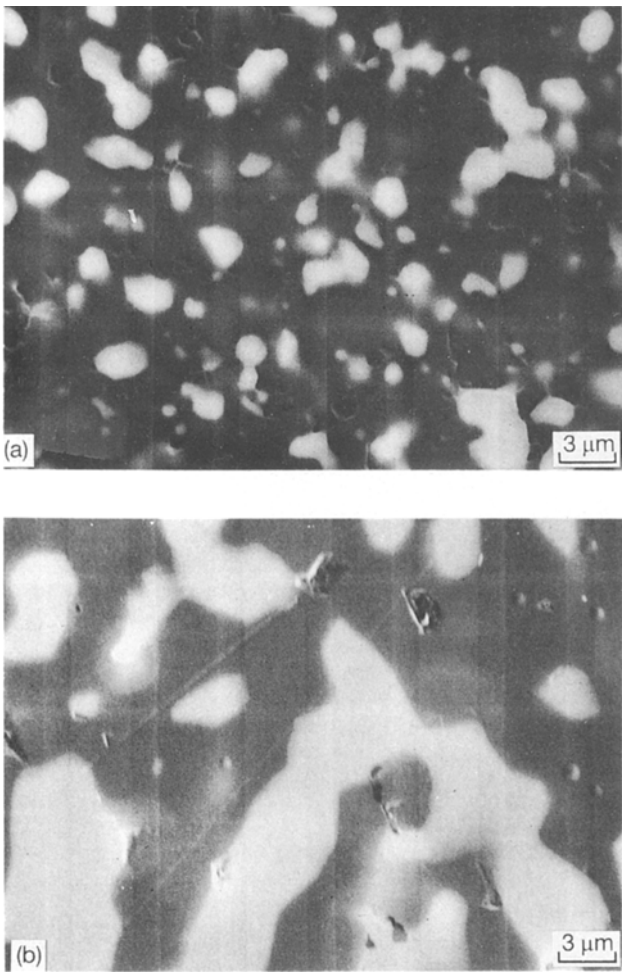

Figure 2 SEM micrographs of 30 vol % Cr_3C_2 (1.5 μm particle size) reinforced Al_2O_3 matrix composites hot-pressed at (a) 1400, (b) 1700 °C. White particles are Cr_3C_2 distributed in grey Al_2O_3 matrix.

The second phase can pin the grain boundary of the matrix phase and inhibit matrix grain growth. The average grain size of Al_2O_3 gradually decreases with increasing Cr_3C_2 content. The average Al_2O_3 grain size for 10 and 40 vol % Cr_3C_2 content is 2.2 and 1.8 μm, respectively, when the sintering temperature is 1400 °C. It is apparent that the Cr_3C_2 particles are more effective in inhibiting the Al_2O_3 grain growth when the sintering temperature rises to 1700 °C, as demonstrated in Fig. 4. The location of Cr_3C_2 particles relative to Al_2O_3 grain is significantly dependent on the particle size and content of Cr_3C_2 in composites. The TEM micrographs of the dense composites sintered at 1400 °C with three sizes of Cr_3C_2 powder (0.5, 1.5 and 7.5 μm) are shown in Fig. 5a–c, respectively. If the particle size of Cr_3C_2 powder is fine, it is easy to see that the Cr_3C_2 particles are trapped within Al_2O_3 grains after sintering shown in Fig. 5a. Similar microstructures of fine second-phase (< 0.3 μm) embedded in the matrix grain can also be found in Al_2O_3 with ZrO_2 [14] and SiC [15, 16] systems. According to Zener's rule [17], the second phase at the grain boundary inserts a dragging force to retard the migration of grain boundaries. The magnitude of this dragging force is proportional to the diameter of the second phase. For fine Cr_3C_2 particles, it can easily detach itself from the boundary. Typical

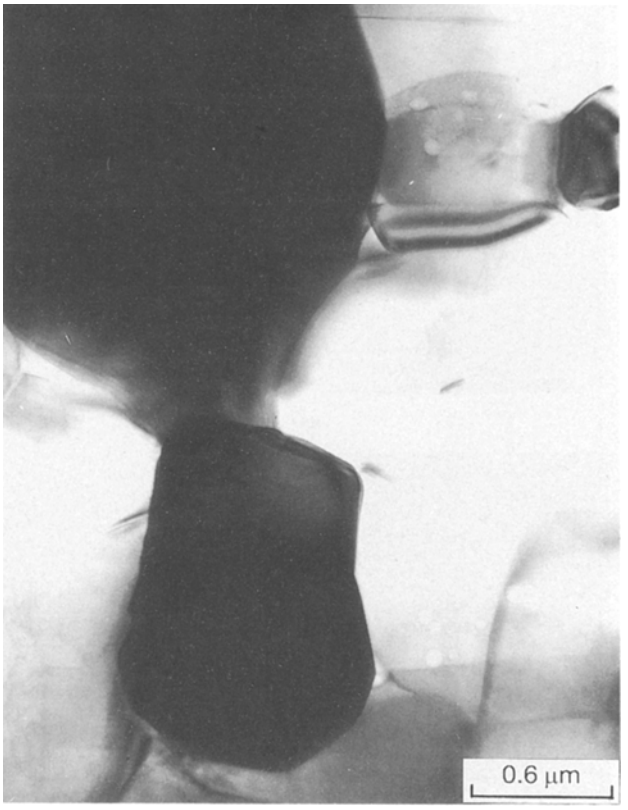

Figure 3 TEM micrographs of 40 vol % Cr_3C_2 reinforced Al_2O_3 composites hot-pressed at 1400 °C. The necking formed by the coalescence of two black Cr_3C_2 particle is shown along the Al_2O_3 grain boundary.

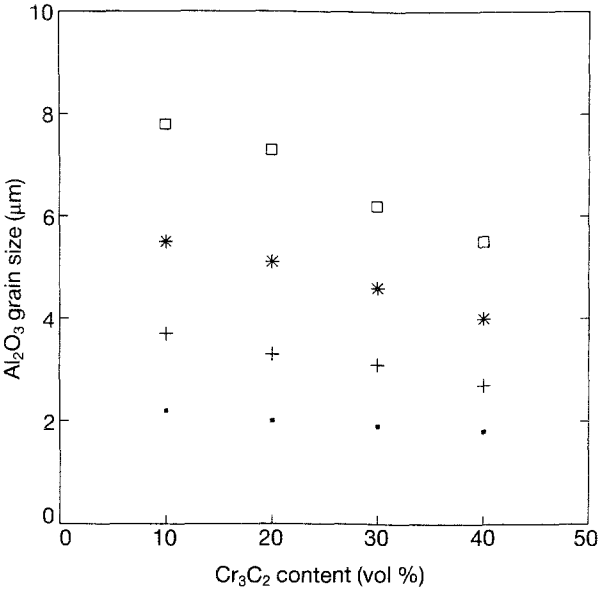

Figure 4 Average Al_2O_3 grain size is dependent on Cr_3C_2 content for Al_2O_3–Cr_3C_2 composites hot-pressed at ~ 1400 °C–1700 °C. HP at ■, 1400; +, 1500; ∗, 1600; □, 1700 °C.

TEM microstructures for the coarser Cr_3C_2 powders (e.g. 1.5 and 7.5 μm) are shown in Fig. 5b and c, respectively. In this case, the Cr_3C_2 particle size is equivalent to or larger than the Al_2O_3 grain size, and a Cr_3C_2 particle is surrounded by several Al_2O_3 grains. According to earlier studies [18, 19] of toughening mechanisms for non-transformation ceramic composites, it is very important for the selected reinforcements not to react chemically with the matrix in order

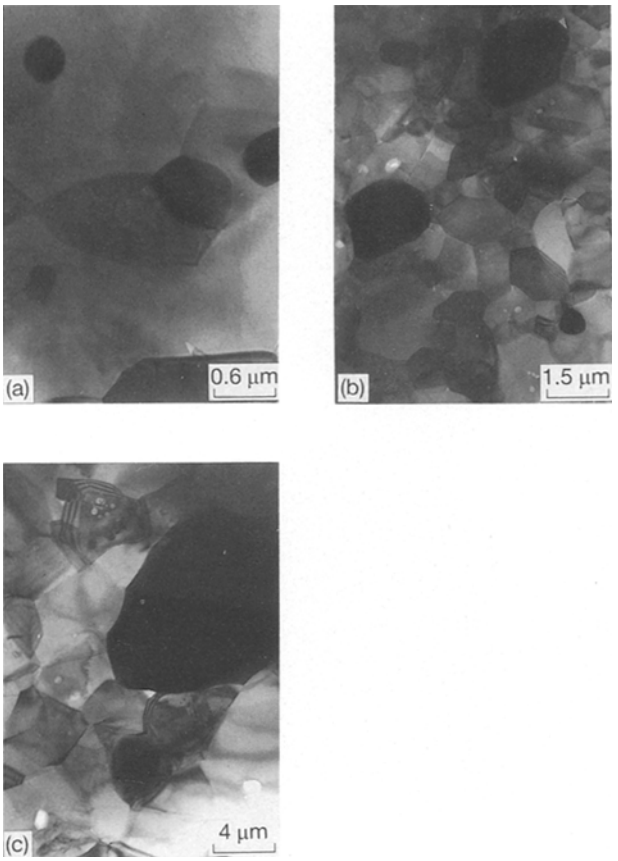

Figure 5 TEM micrographs shows the location of Cr_3C_2 relative to the Al_2O_3 matrix grain in 10 vol % Cr_3C_2/Al_2O_3 composites, incorporated with three grades of Cr_3C_2 particle size. (a) 0.5 μm Cr_3C_2 particle size, Cr_3C_2 particles intragranular Al_2O_3 grain. (b) 1.5 μm Cr_3C_2 particle size, Cr_3C_2 particle size similar to Al_2O_3 grain and surrounded by several Al_2O_3 grains. (c) 7.5 μm Cr_3C_2 particle size, Cr_3C_2 particle much larger than Al_2O_3 grain and surrounded by several Al_2O_3 grains.

to give a high toughness composite. Therefore it is necessary to investigate further the possible interfacial reactions in the Al_2O_3–Cr_3C_2 composite system. X-ray diffraction (XRD) analysis of hot-pressed composites indicated that there is no chemical reaction between Cr_3C_2 and Al_2O_3. A TEM micrograph of an interface between Al_2O_3 and Cr_3C_2 is shown in Fig. 6. There is no evidence for a reaction layer in the interface. Thus the constituents of Cr_3C_2 and Al_2O_3 are chemically compatible during the hot-pressing process. Although the Cr_3C_2 particles coarsen (see Fig. 2) when the hot-pressing temperature rises from 1400 to 1700 °C, the cracks induced by the Vickers' indentor always propagate along the Cr_3C_2–Al_2O_3 interface, shown in Fig. 7a, b, respectively. Thus the weak interfacial bonding between Cr_3C_2 and Al_2O_3 facilitates the debonding process and enhances the fracture resistance/toughness of the composites [18, 19].

3.2. Mechanical properties

Fracture strength data for the densified composites with three kinds of Cr_3C_2 particle size are given in Fig. 8 as a function of Cr_3C_2 content. Let us initially consider the composites when hot-pressed at 1400 °C and with a relative density > 98.5%. The fracture strength of all Al_2O_3/Cr_3C_2 composites hot-pressed at 1400 °C is always higher than for monolithic Al_2O_3

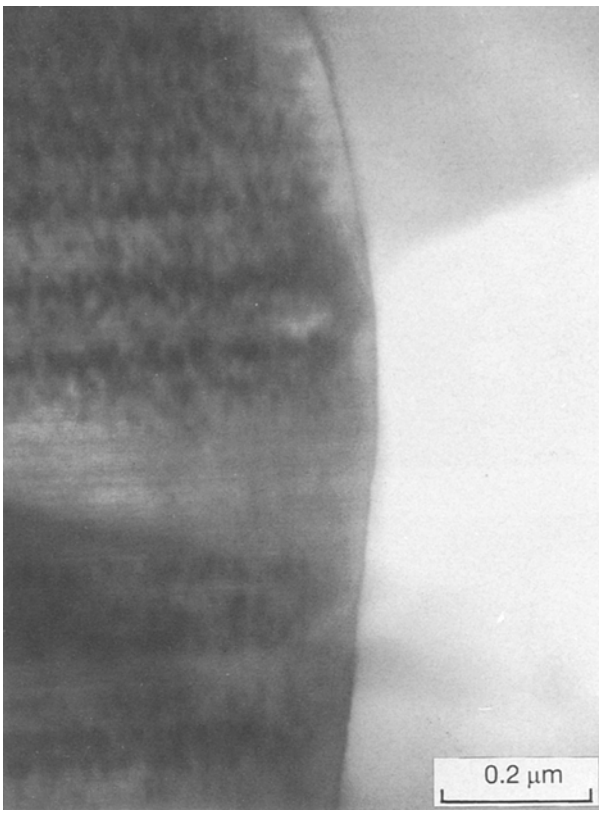

Figure 6 TEM micrograph showing interface between Cr_3C_2 (black) and Al_2O_3 (white). The interface is no evident reacted layer.

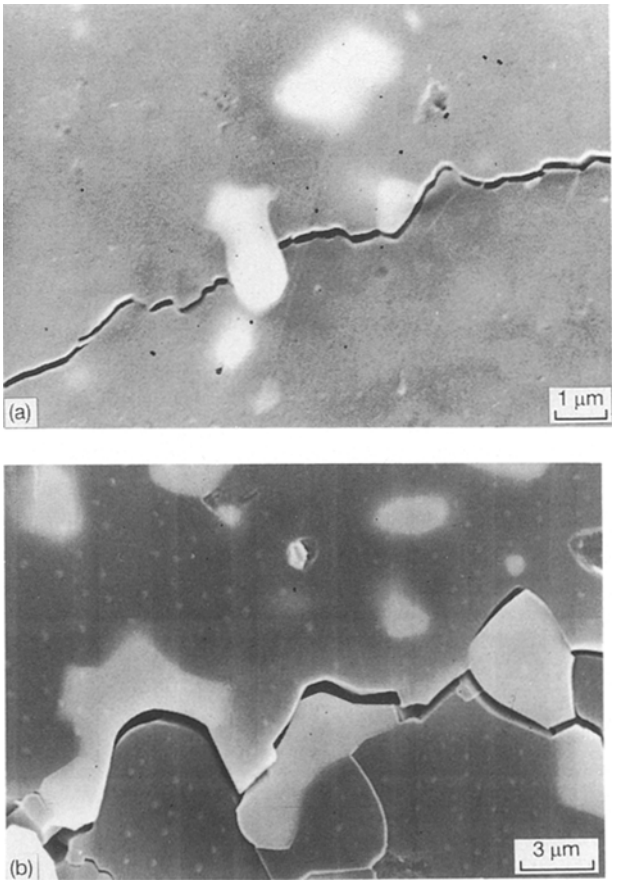

Figure 7 SEM micrographs illustrate the interaction between microcracks induced by Vicker's indentor and Cr_3C_2 particle in 20 vol % Cr_3C_2/Al_2O_3 composites hot-pressed at (a)1400, (b)1700 °C. Microcracks always propagate along Cr_3C_2/Al_2O_3 interface, and a deflection and bridging effect is observed.

(~ 380 MPa). These results indicate that the incorporation of Cr_3C_2 particles into Al_2O_3 matrix can significantly enhance the strength of pure Al_2O_3. For composites using the fine (0.5 μm) Cr_3C_2 powder, the fracture strength significantly increases with Cr_3C_2 content and ranges from 620 to 805 MPa for 10 and 30 vol % Cr_3C_2 content, respectively. Then the strength drops slightly to 785 MPa for 40 vol % Cr_3C_2/Al_2O_3 composites. In contrast, for composites reinforced by medium-sized (1.5 μm) Cr_3C_2 particles, the fracture strength is almost independent of Cr_3C_2 content, with a value of around 610 MPa. For composites incorporating coarse (7.5 μm) Cr_3C_2 particles into the Al_2O_3 matrix, the fracture strength reduces with Cr_3C_2 content and ranges from 780 to 530 MPa for 10 and 40 vol % Cr_3C_2 content, respectively. The fracture surfaces of Al_2O_3/Cr_3C_2 composites containing 0.5, 1.5 and 7.5 μm Cr_3C_2 particles and hot-pressed at 1400 °C are illustrated in Fig. 9a–c, respectively. The fracture mode of composites evidently changes from a mixed mode (transgranular and intergranular, Fig. 9b) to the almost transgranular mode (Fig. 9a) when the particle size of Cr_3C_2 is 0.5 μm instead of 1.5 μm. It may be thought that the change of fracture mode is caused by the different location of Cr_3C_2 particle relative to Al_2O_3 matrix grain. According to the published literature, the fracture strength associated with the transgranular fracture mode is always greater than that of the intergranular fracture mode for monolithic Al_2O_3 [20, 21] or Al_2O_3 matrix composites [15, 16]. An important factor, namely the residual stress, is generated from the large thermal expansion mismatch. The thermal expansion coefficient (TEC) of Cr_3C_2 (11.8×10^{-6} $°C^{-1}$) is greater than that of Al_2O_3 (8.8×10^{-6} $°C^{-1}$); the magnitude and direction of thermal residual stress at the interface which develop during cooling down from the fabricated temperature have been evaluated [22]. The compressive residual stress acting on the Al_2O_3 matrix in the hoop direction is 1250 MPa, but a tensile residual stress acts on the interface in the radial direction. Both the transgranular fracture mode and the great compressive stress in the Al_2O_3 matrix give a high fracture strength for the fine (0.5 μm) Cr_3C_2 particle-reinforced Al_2O_3 composites. It is not feasible for the compressive residual stress to enhance the strength if the paths of crack propagation are intergranular. The magnitude of the residual tensile stress in the radial direction is a triple-order function of the Cr_3C_2 particle size [22]. When 2 μm Cr_3C_2 particles are used, the particle size of Cr_3C_2 is fairly close to the grain size of Al_2O_3 (see Fig. 5b). In addition, the fracture mode changes from transgranular dominantly to mixed, and the greater tensile stress at the interface can reduce the strength from 785 to 610 MPa as the particle size of Cr_3C_2 used in the composites increases from 0.5 to 1.5 μm. When the Cr_3C_2 particle size is coarse (7.5 μm), the fracture mode reverts to the transgranular fracture of the Al_2O_3 matrix, neighbouring the Cr_3C_2 particle, as shown in Fig. 9c. In this case, the particle size of Cr_3C_2 is much greater than the Al_2O_3 grain size (about 2 μm) (see Fig. 5c). The large residual tensile stress becomes the dominant factor in controlling the crack propagating path, and the path changes to transgranular. The fracture strength of coarse Cr_3C_2/Al_2O_3 composites drops with the Cr_3C_2 content because the detrimental effect of residual tensile stress at the interface becomes more apparent with the higher Cr_3C_2 content. The strength of medium Cr_3C_2/Al_2O_3 composite drops to about 430 MPa, as the hot-pressed temperature is increased to 1500 °C. In addition to the almost intergranular fracture (shown in Fig. 9d) in the Al_2O_3 matrix caused by the larger Al_2O_3 grains, the greater tensile stress at the interface and the coalescence of the Cr_3C_2 particle also contribute to a reduction in strength of composites hot-pressed at 1500 °C.

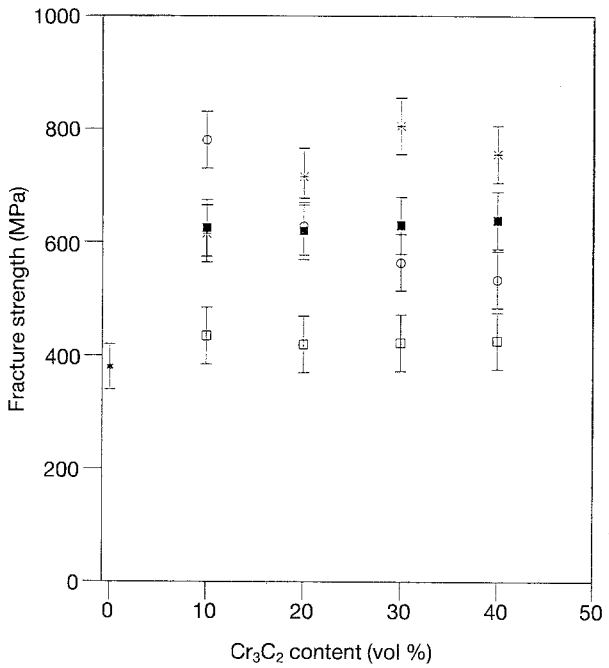

Figure 8 Fracture strength of Al_2O_3–Cr_3C_2 composites is dependent on Cr_3C_2 content and particle size. ■, 1400 °C, 1.5 μm; ○, 1400 °C, 7.5 μm; *, 1400 °C, 0.5 μm; □, 1500 °C, 1.5 μm; ★, Al_2O_3.

The fracture toughness of the composites is presented in Fig. 10 as a function of Cr_3C_2 content. For the medium and coarse Cr_3C_2 particle-reinforced Al_2O_3 composites, the fracture toughness initially increases with Cr_3C_2 content and gives a peak value at 7.5 and 8.0 MPa $m^{1/2}$ of 20 and 30 vol % Cr_3C_2 content, respectively. For the fine-particle Cr_3C_2/Al_2O_3 composites, the fracture toughness remains almost constant at a value of ~ 5.9 MPa $m^{1/2}$. The interactions between Cr_3C_2 particles and microcracks induced by the Vickers' indentor have been shown in Fig. 7. It is apparent that the primary toughening mechanisms are crack bridging and deflection. According to mechanical analysis of the bridging model for the strong particle- [23] or whisker- [18, 19] reinforced ceramic matrix composites, the effect of toughening is proportional to the diameter of the reinforced phase. The coarser reinforced particulate can provide a longer debonding length and greater crack-opening displacements, and thus achieve better toughening. The fracture toughness of the medium-particle Cr_3C_2/Al_2O_3 composites drops from 7.5 to 5.1 MPa $m^{1/2}$ as the hot-pressing temperature is

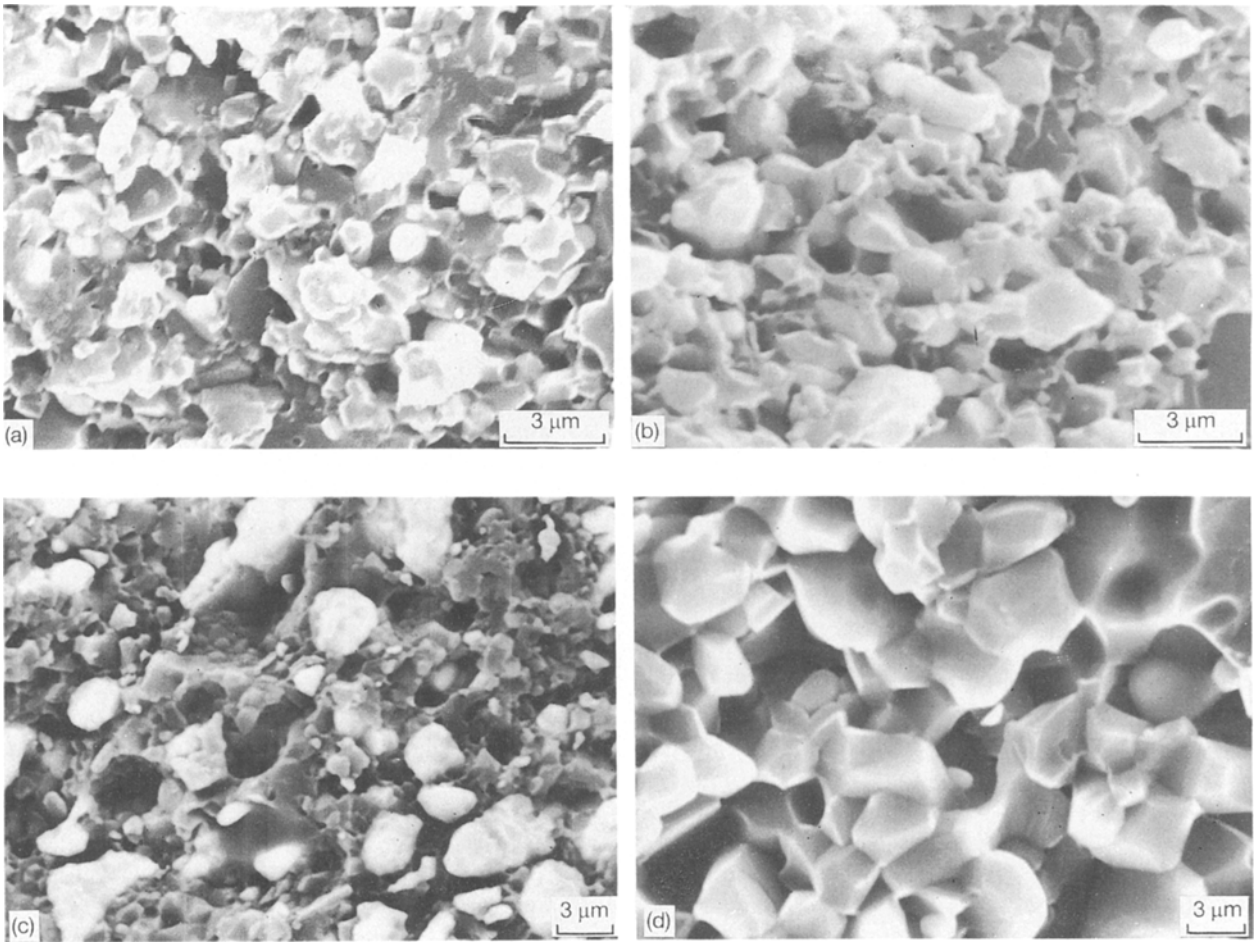

Figure 9 Fracture surface of Al_2O_3–Cr_3C_2 composites with different Cr_3C_2 particle size (D) and hot-pressed temperature (T). (a) Transgranular fracture, $D = 0.5$ μm, $T = 1400$ °C. (b) Mixing fracture mode, $D = 1.5$ μm, $T = 1400$ °C. (c) Transgranular fracture, $D = 7.5$ μm, $T = 1400$ °C. (d) Intergranular fracture, $D = 1.5$ μm, $T = 1500$ °C.

increased from 1400 to 1500 °C. A possible reason is that the coalescence of Cr_3C_2 particles may weaken the interfacial bonding the diffusion of impurities or defects to the interface, to decrease the total energy [19] when the hot-pressing temperature is raised to 1500 °C. Indirect confirmation of this hypothesis was obtained by chemical etching in hot phosphoric acid. It took 40 min and 1.5 h to reveal the Cr_3C_2/Cr_3C_2 and Al_2O_3/Al_2O_3 grain boundaries, respectively, for the composites hot-pressed at 1400 °C, whereas the corresponding times for the composites hot-pressed at 1500 °C were only 20 and 50 min, respectively, due to the higher concentrations of defects or impurities at grain boundary. As the interfacial bonding is too weak, the resistance of the crack propagating along Cr_3C_2/Al_2O_3 is remarkably reduced and the toughening effect is diminished [24]. Although the grain size of Al_2O_3 matrix is a little larger, which enhances toughness by matrix grain bridging [18, 25], the net toughness is significantly deteriorated by the weakening of the interfacial bond as the hot-pressing temperature rises from 1400 to 1500 °C.

3.3. Electrical conductivity

The electrical conductivity of the medium-particle Cr_3C_2/Al_2O_3 composites hot-pressed at temperatures in the range 1400 to 1700 °C is shown in Fig. 11 as a function of Cr_3C_2 content. As the electrical conductivity of Cr_3C_2 ($68 \times 10^6\ \Omega^{-1}\ cm^{-1}$) is much higher than that of Al_2O_3 ($10^{-14}\ \Omega^{-1}\ cm^{-1}$), the electrical conductivity of the composites drastically increases with the Cr_3C_2 content. According to the percolation theory [26, 27], an electrical current flows selectively through the connections of conductive particles when both the insulated particles and the conductive particles are mixed. The critical volume of the conductive phase is inversely proportional to the particle size of the conductive particle when the conductive channel is formed. Therefore the lower conductivity of the composites densified at the higher temperature is caused by the coalescence of Cr_3C_2 particles [Fig. 11]. Electrical discharge machining (EDM) experiments were conducted on the Al_2O_3-based composites with ~ 10–40 vol % Cr_3C_2 content. For all the 10 and 20 vol % Cr_3C_2/Al_2O_3 composites, EDM cannot be performed as no electrical arcs are produced between the specimens and the wire. For the 30 vol % Cr_3C_2/Al_2O_3 composites, excluding one hot-pressed at 1700 °C, and all the 40 vol % Cr_3C_2/Al_2O_3 composites, EDM can be performed in the Castrol SPE oil sinker. According to the wire EDM experimental results, machining by EDM is possible for Al_2O_3–Cr_3C_2 composites with an electrical conductivity higher than $25\ \Omega^{-1}\ cm^{-1}$. The limiting value is very close to published experimental results [6] that

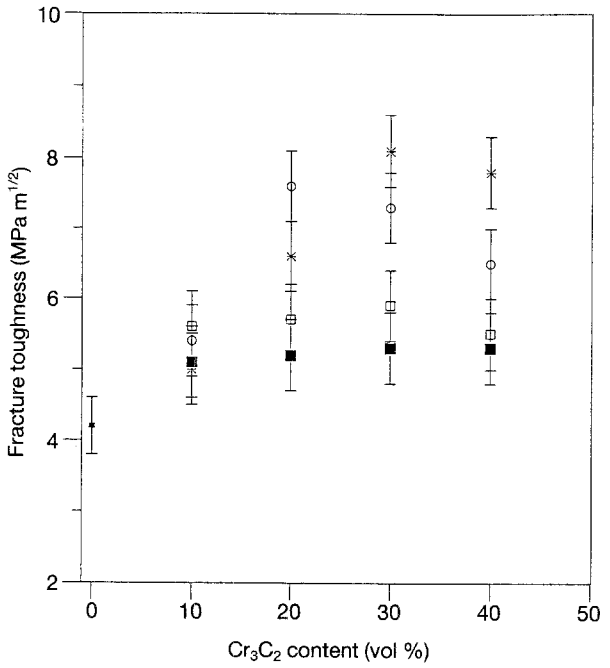

Figure 10 Fracture toughness of Al_2O_3–Cr_3C_2 composites is dependent on the Cr_3C_2 content and particle size. ○, 1400 °C, 1.5 μm; *, 1400 °C, 7.5 μm; □, 1400 °C, 0.5 μm; ■, 1500 °C, 1.5 μm; ★, Al_2O_3.

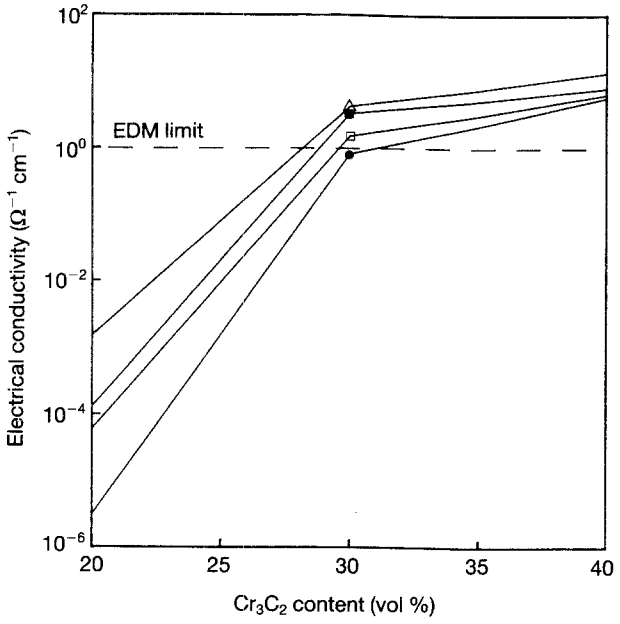

Figure 11 Electrical conductivity of Cr_3C_2(M)/Al_2O_3 composites is dependent on the Cr_3C_2 content and hot-pressed temperatures. Dashed line indicates limited electrical conductivity of Al_2O_3 matrix composites for EDM. △, 1400; ■, 1500; □, 1600; ●, 1700 °C.

the limiting value for Al_2O_3-based composites reinforced by TiC and TiN particles is 1 Ω^{-1} cm^{-1}.

4. Conclusions

The Al_2O_3–Cr_3C_2 composites can be densified by hot pressing at 1400 °C to > 98.5% relative density. The addition of Cr_3C_2 particles to the Al_2O_3 matrix can retard the densification and inhibit the grain growth of the Al_2O_3 matrix. It has been demonstrated that the incorporation of Cr_3C_2 particles can effectively strengthen and toughen the Al_2O_3 matrix. This toughening effect is mainly due to the crack bridging and deflection mechanisms. The transgranular fracture mode and residual compressive stress are the primary strengthening mechanisms. The electrical conductivity of Al_2O_3 matrix can be much improved by the addition of higher conductive Cr_3C_2 particles. The EDM method can be performed as the electrical conductivity of Al_2O_3–Cr_3C_2 composites is greater than 25 Ω^{-1} cm^{-1}.

Acknowledgement

The authors would like to thank the Ministry of Economic Affairs of The Republic of China for financial support under the contract No. Mat. 38P3210.

References

1. R. A. CUTLER and K. M. RIGTRUP, *J. Amer. Ceram. Soc.* **75** (1992) 36.
2. C. H. JUNG and C. H. KIM, *J. Mater. Sci.* **26** (1991) 5037.
3. M. BENGISU and O. T. INAL, *Ceram. Int.* **17** (1991) 187.
4. R. A. CUTLER and A. C. HURFORD, *Mater. Sci. Engng*, **A105/106** (1988) 183.
5. N. F. PETROFES and A. M. GADALLA, *Amer. Ceram. Soc. Bull.* **67** (1988) 1048.
6. B. CALES, C. MARTIN and P.VIVIER, in Proceedings of the Third International Symposium of Ceramic Materials and Components for Engines, Las Vegas, Nevada, November 1988, edited by V. J. Tennery (The American Ceramic Society, Westerville, OH, 1989) p. 1189.
7. A. BELLOSI, G. D. PORTU and S. GUICCIARDI, *J. Eur. Ceram. Soc.* **10** (1992) 307.
8. E. KLAR, in "Metals Handbook", 9th edition, Vol. 7 (American Society for Metals, Metals Park, Ohio, 1984) p. 804.
9. M. ANDO and H. AWAJI, *Taikabutsu* **41** (1989) 239.
10. F. F. LANGE, *J. Mater. Res.* **2** (1987) 59.
11. R. K. BORDIA and G. W. SCHERER, *Acta Metall.* **36** (1988) 2393.
12. S. SUNDARESAN and L. A. AKSAY, *J. Amer. Ceram. Soc.* **73** (1990) 54.
13. J. WANG and R. RAJ, *ibid.* **74** (1991) 1959.
14. F. F. LANGE and M. M. HIRLINGER, *ibid.* **67** (1984) 164.
15. K. NIIHARA, A. NAKAHIRA and M. INOVE, in "Better Ceramics Through Chemistry", edited by M. J. Hampdensmith, W. G. Klemperer and C. J. Brinker (Materials Research Society Symposium Proceedings, Vol. 271, Pittsburgh, P.A., 1992) p. 589.
16. L. C. STEARNS, J. ZHAO and M. P. HARMER, *J. Eur. Ceram. Soc.* **10** (1992) 473.
17. C. S. SMITH, *Trans. Metall. Soc. AIME* **175** (1949) 15.
18. P. F. BECHER, *J. Amer. Ceram. Soc.* **74** (1991) 255.
19. A. G. EVANS, *ibid.* **73** (1990) 187.
20. R. W. DAVIDGE, in "Fracture Mechanics of Ceramics", Vol. 4, edited by R. C. Bradt, A. G. Evans, D. P. H. Hasselman and F. F. Lange (Plenum, New York, 1978) p. 447.
21. P. L. GUTSHALL and G. E. GROSS, *Eng. Frac. Mech.* **1** (1969) 463.
22. W. D. KINGERY, H. K. BOWEN and D. R. UHLMANN, "Introduction to Ceramics" (Wiley, New York, 1976) p. 177.
23. A. G. EVANS and R. M. MCMEEKING, *Acta Metall* **34** (1986) 2435.
24. F. ERDOGAN and P. F. JOSEPH, *J. Amer. Ceram. Soc.* **72** (1989) 262.
25. P. F. BECHER, C. H. HSUEH, P. ANGELINI and T. N. TIEGS, *ibid.* **71** (1988) 1050.
26. D. R. CLARKE, *ibid.* **75** (1992) 739.
27. G. RAJAGOPAL and M. SATYAM, *J. Appl. Phys.* **49** (1978) 5536.

Received 29 April
and accepted 6 October 1993